the abundance of HCO^+ decreases by a factor of ~ 20 (Iglesias & Silk, 1978). The derived $[HCO^+]/[CO]$ ratios in the lobes of Sandqvist 136 then give further support to the notion that the abundances in the lobes are a product of shock chemistry.

In addition to the wing emission detected toward the lobes of Sandqvist 136 in the lines of SiO and CH_3OH, we note the presence of emission at velocities comparable to the systemic velocity of the globule. In particular for silicon monoxide, emission in the velocity range of the ambient cloud is observed only at the position of the lobes. This can be appreciated in Figure 6 which shows velocity-position diagrams of the emission in the SiO lines along the symmetry axis of the outflow. The strength of the emission in the red lobe is roughly constant with velocity, with peaks at –4.1 and –0.8 km s^{-1}, while in the blue lobe the emission peaks at a velocity of –5.0 km s^{-1}, close to the ambient cloud velocity. This result suggests that the enhancement of SiO and CH_3OH molecules might be due to two different processes: heating of grains within the ambient core medium by the UV radiation produced in the shocks, which can evaporate volatile grain mantles and trigger gas-phase reactions, and direct shock processing of dust located within the shocked region. The low velocity emission would then arise from pre-shock gas heated by the radiation from the hot post-shock gas, while the high velocity emission arises from the cold post shock gas.

Conclusions and Outlook

Multiline molecular observations toward the Sandqvist 136 dark globule have revealed a spectacular enhancement in the abundance of silicon monoxide and methanol molecules at the lobes of the associated bipolar outflow. The spatial distribution and broad line profiles of the SiO and CH_3OH emission indicates a common mechanisms for the excitation of these lines: shocks. We conclude that the shocks created by the interaction between flows and the surrounding medium play a major role in the production of these molecules. In particular the strong emission observed in the methanol lines suggest that these lines can be used as powerful signposts of the chemical impact of bipolar outflows on the surrounding ambient medium. It appears that the Sandqvist 136 shock produces the evaporation of icy grain mantles resulting in the injection into the gas phase of large amount of ice mantle constituents, such as methanol. Further, the shock seems to be sufficiently powerful that refractory dust grains are partially destroyed, liberating into the gas phase a significant amount of Si atoms that are later converted to SiO by ion-molecule reactions and/or shock chemistry. Finally, we find that the SiO and CH3OH emission detected toward the lobes not only traces shocked outflowing gas but also ambient medium gas that has been heated by the UV radiation from the hot post shock regions.

It has been suggested that the strength of the emission in diverse trace molecules might be considered an indicator of the evolutionary stage of bipolar outflows (Bachiller & Gómez-González, 1992). It would appear that the profuse emission observed in the lines of methanol and silicon monoxide from the Sandqvist 136 outflow implies that we are witnessing an early stage of the outflow phase in which molecules in icy mantles and atoms in dust grains are efficiently liberated back into the gas phase. How much of the enhancement factor depends on wind velocity and/or on evolutionary age has not, however, yet been established. The determination of the abundance of more complex organic molecules in the lobes, such as CH_3OCH_3, $HCOOCH_3$, and CH_3CN, which can potentially serve as clocks of the evolutionary state of the outflows (van Dishoeck & Blake, 1995), should be obtained to provide answer to these questions.

References

André, P. 1995, *Astr. & Spa. Sci.* **224**, 29.
André, P., Martín-Pintado, J., Despois, D., & Montmerle, T. 1990, *A&A* **236**, 180.
Bachiller, R., Cernicharo, J., Martín-Pintado, J., Tafalla, M., & Lazareff, B. 1990, *A&A* **231**, 174.
Bachiller, R., Fuente, A., & Tafalla, M., 1995, *ApJ* **445**, L51.
Bachiller, R., & Gómez-González, J. 1992, *A&AR* **3**, 257.
Bachiller, R., Liechti, S., Walmsley, C.M., & Colomer, F. 1995, A&A **295**, L51.
Bachiller, R., Martín-Pintado, J., & Fuente, A. 1991, *A&A* **243**, L21.
Bally, J., & Lada, C.J. 1983, *ApJ* **265**, 824.
Bally, J., Lada, E., & Lane, A.D. 1993, *ApJ* **418**, 322.
Bourke, T.L., Garay, G., Lehtinen, K.K., Köhnenkamp, I., Launhardt, R., Nyman, L.-A., May, J., Robinson, G., & Hyland, A.R. 1996, *ApJ* submitted.
Bourke, T.L., Hyland, A.R., Robinson, G., James, S.D., & Wright, C.M. 1995, *MNRAS* **276**, 1067.
Charnley, S.B., Tielens, A.G.G.M., & Millar, T.J. 1992, *ApJ* **399**, L71.
Fukui, Y., Iwata, T., Mizuno, A., Bally, J., & Lane, A.P. 1993, in *Protostars and Planets III*, eds. E.H. Levy & J. Lunine (Tucson: Univ. Arizona Press), 603.
Lada, C.J. 1985, *ARA&A* **23**, 267.
Lada, C.J., & Fich, M. 1996, *ApJ* in press.
Hartquist, T.W., Oppenheimer, M., & Dalgarno, A. 1980, *ApJ* **236**, 182.
Iglesias, E.R. & Silk, J. 1978, *ApJ* **226**, 851.
Martín-Pintado, J., Bachiller, R., & Fuente, A. 1992, *A&A* **254**, 315.
Mikami, H., Umemoto, T., Yamamoto, S., & Saito, S. 1992, *ApJ* **392**, L87.
Millar, T.J., Herbst, E., & Charnley, S.B. 1991, *ApJ* **369**, 147.
Mitchell, G.F. 1987, in Astrochemistry, IAU Symposium No. 120, 275.
Mundt, R. 1988, in *Formation and Evolution of Low Mass Stars*, eds. A.K. Dupree and M.T.V.T. Lago, 257.
Neufeld, D.A., & Dalgarno, A. 1989 *ApJ* **340**, 869.
Raga, A., & Cabrit, S. 1993, *A&A* **278**, 267.
Reipurth, B. 1991, in *The Physics of Star Formation and Early Stellar Evolution*, eds. C.J. Lada and N.D. Kylafis, 497.
Rodríguez, L.F., Ho, P.T.P., & Moran, J.M. 1980 *ApJ* **240**, L149.
Sandqvist, A. 1977, *A&A* **57**, 467.
Snell, R.L., Loren, R.B., & Plambeck, R.L. 1980, *ApJ* **239**, L17 .
Turner, J.L., & Dalgarno, A. 1977, *ApJ* **213**, 386.
van Dishoeck, E.F. & Blake, G.A. 1995, *Astr. & Spa. Sci.* **224**, 237.
van Dishoeck, E.F., Blake, G.A., Draine, B.T., & Lunine, J.I. 1993, in *Protostars and Planets III*, eds. E.H. Levy & J.I. Lunine (Tucson: Univ. Arizona Press), 163.
Zhang, Q., Ho, P.T.P., Wright, M.C.H., & Wilner, D.J. 1995, *ApJ* **451**, L71.

E-mail address:
guido@calan.das.uchile.cl (Guido Garay)

On the Optical Emission of the Crab Pulsar

E.P. NASUTI[1,3], R. MIGNANI[1], P.A. CARAVEO[1] and G.F. BIGNAMI[1,2]

[1]Istituto di Fisica Cosmica del CNR, Milan, Italy; [2]Dipartimento di Ingegneria Industriale, Università di Cassino, Italy; [3]Università degli Studi di Milano, Italy

1. Introduction

The Crab Pulsar (PSR0531 +21) was the first Isolated Neutron Star (INS) detected at optical wavelengths. It is identified with a star (V ~ 16.5) near the centre of the Crab Nebula, the remnant of the supernova explosion observed in the summer of 1054. The identification has been confirmed by the discovery of pulsed optical emission at the radio period (Cocke et al., 1969).

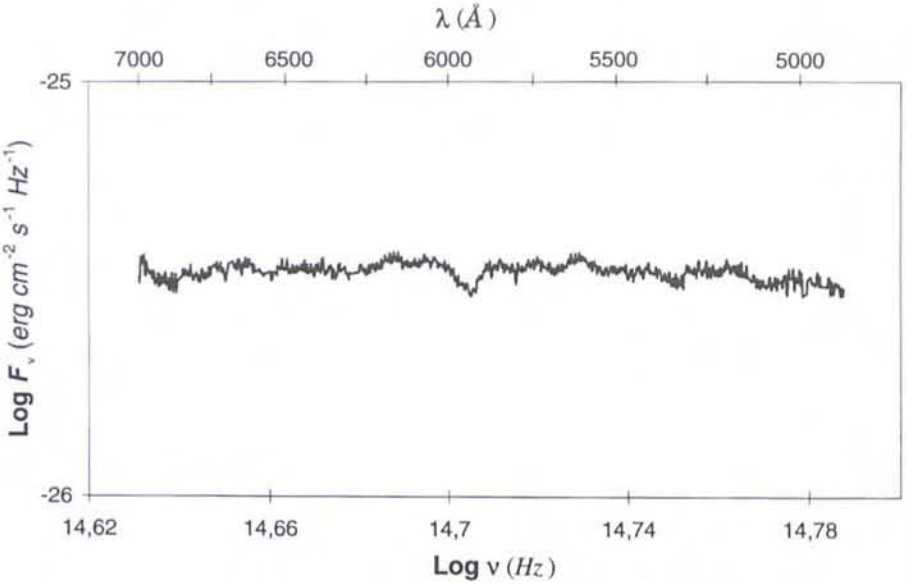

Figure 1: Spectrum of the Crab Pulsar in the wavelength range 4900– 7000 Å as measured with EMMI after a 40-min exposure. The spectrum has been sky subtracted and corrected for interstellar absorption. The flux distribution is modelled by a power law with a best fitting spectral index $\alpha = -0.10 \pm 0.01$. A broad ($\Delta\lambda \sim 100$ Å) absorption feature centred on $\lambda = 5900$ Å is visible.

For almost 10 years, the Crab was the only INS seen at optical wavelength. The Vela pulsar was observed in 1976 (Lasker, 1976) and PSR0540-69 in 1985 (Middleditch and Pennypacker, 1985). Thus, it appears natural that the Crab was used as a test case for the understanding of the optical, nonthermal emission from pulsars. The original model of Pacini (1971) explains the optical emission of young pulsars as synchrotron or curvature radiation produced by energetic particles moving in the pulsar magnetosphere, close to the light cylinder. As a result, a simple dependence is found between the optical emission and the pulsar's key parameters. In particular, the bolometric luminosity should scale with B^4P^{-10} where B is the pulsar's magnetic field and P is the period. Using the Crab as a reference, this law was used by Pacini (1971) to predict the optical luminosity of the Vela pulsar. Indeed, a few years later, the Vela pulsar optical counterpart was detected at the expected magnitude (Lasker, 1976).

The above model also implies a regular decrement of the optical luminosity due to the pulsar's slow down ($L \propto P$). When Kristian (1978) claimed the evidence for the Crab secular decrease, the Pacini's law was considered proved.

Doubts were raised with the discovery of optical pulsations from PSR0540-69 (Middleditch & Pennypacker, 1985), but its apparent overluminosity could be explained revisiting the model for the effects of the pulsar's duty cycle (Pacini & Salvati, 1987). More recently, optical counterparts have been found for Geminga (Bignami et al., 1987) and proposed for PSR0656+14 (Caraveo et al., 1994a) and PSR1509-58 (Caraveo et al., 1994b).

However, the Crab remains by far the brightest of the optically emitting INSs, hundreds of times brighter than PSR054069 (V = 22.4), Vela (V = 23.6) and PSR1509-58 (V = 22) and thousands of times brighter than Geminga (V = 25.5) and PSR0656+14 (V = 25). Therefore, it is the only INS within reach of optical spectroscopy. Nevertheless, our knowledge of the optical spectrum of the Crab Pulsar rests mainly on the pioneering observations of Oke (1969), and on multicolour photometry (Kristian et al., 1970; Middleditch et al., 1987; Percival et al., 1993). Thus, it seemed appropriate to bring the knowledge of the Crab optical emission up to modern astronomy standards.

2. The Observations

A 40-minute spectrum of the Crab Pulsar was taken on January 1991 with the NTT. The telescope was equipped with the ESO Multi Mode Instrument (EMMI) (Melnick, Dekker and D'Odorico, 1991) mounting a "Red" THX 10242 CCD detector. The instrument was operated in the Red Medium Dispersion Mode (REMD), with a projected pixel size of 0.44 arcsec. A medium dispersion grating blazed at 6200 Å was used, providing a spectral resolution of 2.1 Å/pixel in the wavelength range 4900–7000 Å. According to the seeing conditions (~ 1.2 arcsec) the Pulsar was centred in a 1.5 arcsec slit, with the long axis oriented East-West and extending

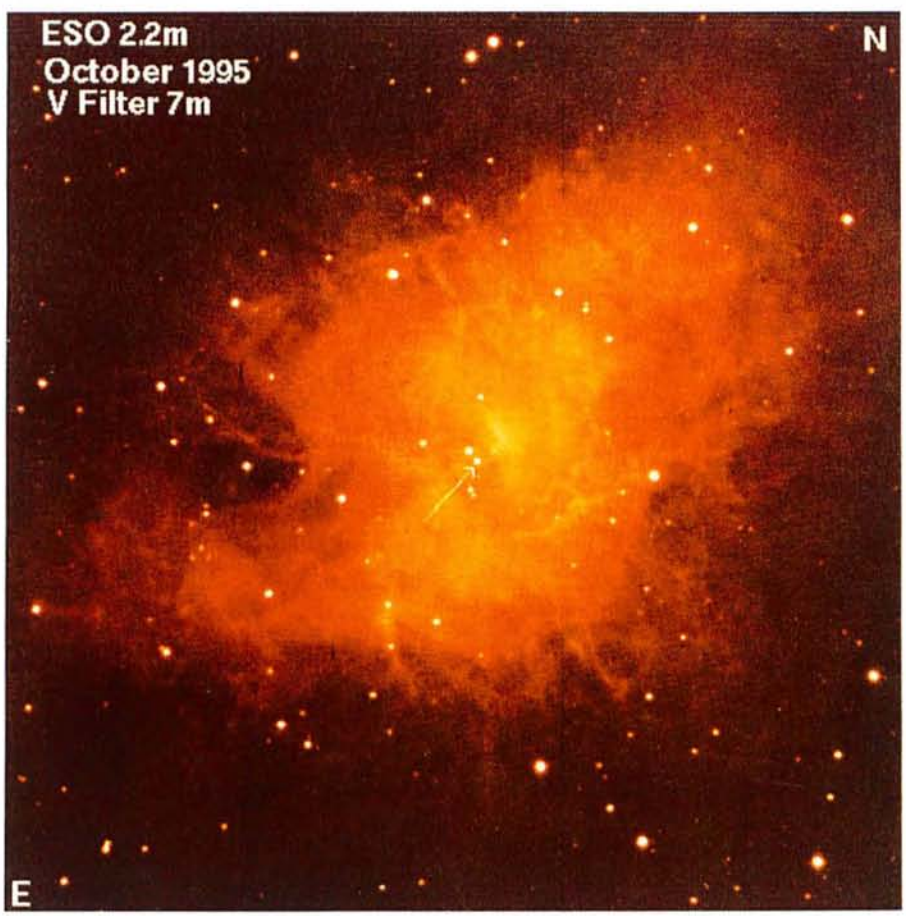

Figure 2: V filter image of the Crab Nebula taken on October 1995 with EFOSC at the ESO 2.2-m. The Crab Pulsar is indicated by the arrow (Courtesy S. Molendi and M.-H. Ulrich).

6 arcmin along the remnant. The two-dimensional spectrum was reduced using the spectral analysis packages LONG and ALICE available in MIDAS. After standard reduction (cosmic ray cleaning, bias subtraction and flat-fielding), the wavelength calibration was performed using the spectrum of an He calibration lamp. After sky-subtraction, a one-dimensional averaged spectrum of the pulsar was extracted. The spectrum was then corrected for the atmospheric extinction (z = 1.61), using standard tables for La Silla available in the ESO database, and flux-calibrated using, as a reference, the spectrum of the standard star Feige 24 (Oke, 1974). To obtain a "clean" spectrum of PSR0531+21, the nebular background was also subtracted. The subtraction of emission/absorption features from the nebula was difficult because of the wavelength scatter induced by the spread in radial velocity of the expanding gas. Residual features in the pulsar spectrum, clearly identified as due to excess or defect of subtraction, were removed. The spectrum was finally corrected for the interstellar extinction using an E(B – V) = 0.51 ± 0.04 (Percival et al., 1993) and the extinction curve of Savage & Mathis (1979).

New photometric observations of the Crab Pulsar have been performed on October 1995 by S. Molendi. 7 one-minute V filter exposures have been collected with EFOSC2 at the ESO 2.2-m telescope (Fig. 2). The seeing was around 0.9 arcsec, with an airmass ~ 1.2. Two 3-minute images of the Stobie field F117-18 (Stobie et al., 1987) have been used to compute the zero point magnitude. The aperture photometry, computed on the average frame, yields a magnitude of 16.72 ± 0.05 for the Crab pulsar, where the uncertainty includes both photometry and calibration errors.

3. The Spectrum

The flux distribution (*logF_ν* vs. *logν*) of the Crab Pulsar is plotted in Figure 1, to be compared with the one reported by Oke (1969) obtained with much scanter data. The spectral shape is well fitted by a flat power law ($F_\nu \propto \nu^\alpha$) with a best fit spectral index $\alpha = -0.10 \pm 0.01$. For comparison, Oke (1969) gave a spectral index $\alpha = -0.2$ with no quoted uncertainty, while Percival et al. (1993), fitting the observed fluxes computed at the peak of U, B and V bands, obtained $\alpha = -0.07 \pm 0.30$. The power law spectral index arising from our spectrum is far more precise than anything available so far.

An interesting, unidentified, absorption feature is visible in the otherwise flat continuum of the pulsar close to λ = 5900 Å. Since the feature is barely recognisable also in the raw data, but not in the spectroscopic flats, we are confident that it is real and not due to a variation in the CCD response. However, we can not exclude that the observed feature is due to a data analysis artifact induced by the interpolation of the rather coarse spectral data available for Feige 24 (which has flux value every 80 Å, i.e. 40 times worse than our spectral data).

The origin of this absorption dip is not very clear. Since this has not been observed in the spectrum of the nebula, it can not be due to absorption by the interstellar medium or the nebula itself. An alternative, more likely, explanation suggests that the absorption takes place very close to the pulsar.

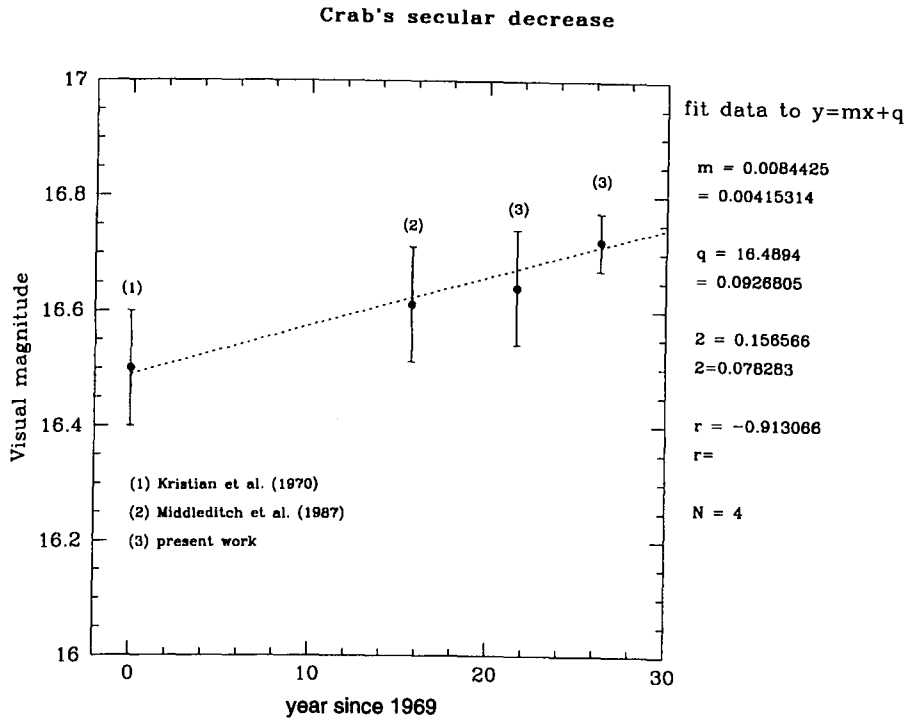

Figure 3: Linear fit of the V magnitudes of the Crab Pulsar vs. time. An apparent correlation is visible, which supports the presence of a decrement in the optical luminosity of the pulsar. The best fitting slope corresponds to a decrement of 0.008 ± 0.004 mag/yr, where the low significance is due to the large errors bars associated with the first three measures.

4. The Secular Decrease

Using the appropriate value for the Crab spin down ($P \sim 4\ 10^{-13}$s s^{-1}) a secular decrease of ~ 0.005 mag/year is expected. A decrement of ~ 0.5%/yr in the optical flux of the Crab pulsar, based on relative photometry measurements, was indeed announced by Kristian (1978), but without mentioning any magnitude value nor any uncertainty. A measure of Crab's magnitude compatible with the expected decrement was later given by Middleditch, Pennypacker and Burns (1987). In order to have a better grasp of the secular decrease, we compared the published values of the Crab V magnitude with the results of our recent observations. We used our photometric point plus the V magnitude obtained integrating the Crab spectrum over the Johnson's V band, and convolving with a model filter response (Bessel, 1990), yielding a value of 16.64 ± 0.1.

In order to investigate the time dependence of the optical luminosity we plotted our values together with previous measurements from Kristian et al. (1970) and Middleditch et al. (1987). To allow a direct comparison, no interstellar extinction correction has been applied to the visual magnitudes. A linear regression to all the available data was then computed. The points in Figure 3 show a significant correlation (~ 90 %), corresponding to a monotomic increase of the visual magnitude with a rate of 0.008 ± 0.004 mag/year i.e. a value certainly in agreement with the theoretical one (~ 0.005 mag/ year), although of limited significance. Actually, the big error bars attached to the first three measures make it difficult to assess the reality of the effect as well as its real magnitude.

5. Conclusions

The first high-quality optical spectrum of the Crab Pulsar has allowed the accurate measurement of the pulsar spectral shape in the visible domain.

While a flat power law ($\alpha = 0.1 \pm 0.01$) describes well the optical spectrum, a dip is found at λ = 5900 Å. Although of unknown origin, it is probably to be associated with the pulsar (or its immediate surroundings) since no evidence for a similar dip is found in the adjacent nebular spectra. More observations are obviously needed to confirm the existence

and to clarify the nature of the absorption feature.

In parallel, the long-term evolution of the optical luminosity of the pulsar has been studied and found to be poorly constrained by the data available so far. Fitting all the available flux measurements as a function of time, we obtain a decrement of 0.008 ± 0.004 mag/yr which is consistent with the expected value of ~ 0.005 mag/yr. However, in view of the error to be attached to the data points, the result is far from conclusive and no claim for a measure of the secular decrease can be put forward at this time. New precise measurements are required to proof the presence of a secular decrease and to quantify its actual value.

Acknowledgements

We are pleased to thank S. Molendi and M.-H. Ulrich who kindly reserved part of their observing run to perform new observations of the Crab.

References

[1] Bessel, M.S.,1990 PA.S.P. **102**, 1181.
[2] Bignami, G.F. et al., 1987 *Ap.J.* **319**, 358.
[3] Caraveo, P.A., Bignami, G.F. and Mereghetti, S., 1994a *Ap.J. Lett.* **422**, L87.
[4] Caraveo, P.A., Mereghetti, S. and Bignami, G.F., 1994b *Ap.J. Lett.* **423**, L125.
[5] Cocke W.J., Disney M.J. e Taylor D.J., 1969, *Nature* **221**, 525.
[6] Kristian, J. et al., 1970, *Ap. J.*, **162**, 475.
[7] Kristian J., 1978, *BAAS*, **10**, 245.
[8] Lasker B.M., 1976 *Ap. J.* **203**, 193.
[9] Melnick J., Dekker H. and D'Odorico S., 1992 *EMMI Operating Manual.*
[10] Middleditch J. and Pennypacker C.,1985 *Nature* **313**,659.
[11] Middleditch J., Pennypacker C. and Burns M.S., 1987 *Ap.J.* **315**, 142.
[12] Oke J.B., 1969, *Ap.J.* **156**, L49.
[13] Pacini F.,1971, *Ap.J.*, **163**, L17.
[14] Pacini F. e Salvati M.,1987, *Ap.J.*, **321**, 447.
[15] Percival J.W. et al., 1993, *Ap. J.*, **407**, 276.
[16] Savage B.D. & Mathis J.S., 1979, *A.R.A.& A.*, **17**, 73.
[17] Stobie, R.S., Sagar, R. and Gilmore, G., 1985 *Astron. Astrophys. Suppl.* **60**, 503.

E-mail address: nasuti@ifctr.mi.cnr.it
(Francesco Nasuti)

2-Micron Images of Titan by Means of Adaptive Optics

M. COMBES, L. VAPILLON, E. GENDRON, A. COUSTENIS and O. LAI

Département de Recherche Spatiale (DESPA), Observatoire de Paris
Unité de Recherche Associée au CNRS (URA 264), Meudon, France

1. Introduction

In this paper we present spatially resolved images of Titan's surface obtained in September 1994, by means of adaptive optics at the ESO 3.6-metre telescope, in narrow-band filters in the near infrared spectral range, defined in such a way that the contribution of the flux reflected by Titan's ground surface is maximised.

Spatially resolved images of Titan would provide significant clues to understand better the controversial nature of Titan's surface. Imaging Titan is a difficult task due to Titan's small angular diameter as seen from Earth (0.8 arcsec). It must be performed in the near infrared since Titan's surface cannot be observed in the visible range due to a uniform and opaque layer of aerosols in Titan's stratosphere.

During the definition phase of the Cassini-Huygens ESA-NASA mission, T. Encrenaz and M. Combes (DESPA, Paris Observatory) and, independently, M. Tomasko, P. Smith and colleagues (Univ. of Arizona) have shown that there must exist transparency windows in Titan's atmosphere where both the molecular absorption and the scattering extinction are sufficiently faint to allow to probe the Titan's surface. This has been confirmed by several authors who observed photometric or spectroscopic fluctuations of Titan's near infrared flux. The most favourable spectral range is in the near infrared around 2.0, 1.6, 1.28, 1.08 and 0.94 micron.

COME-ON+ is the first adaptive optics system devoted to astronomy. It has been developed for ESO by the Space Research Department (DESPA) of Paris Observatory with the collaboration of French companies (ONERA and LASERDOT).

2. Adaptive Optics

The aim of adaptive optics is to correct in real time the phase perturbations induced by the atmospheric turbulence on the incident wavefront reaching the telescope. These perturbations are measured by a wavefront sensor (Fig. 1) using part of the light of the observed source (if quite stellar-like and sufficiently bright) or of a close star in the isoplanetic field (~30 arcsec). Opposite phase corrections are then applied thanks to a thin deformable mirror in a pupil plan (O. Saint Pé et al., 1993, Icarus 105, 263).

The first spatially resolved image of Titan's disk was obtained, in May 1991, by DESPA (O. Saint-Pé, 1993), demonstrating the feasibility of mapping Titan's

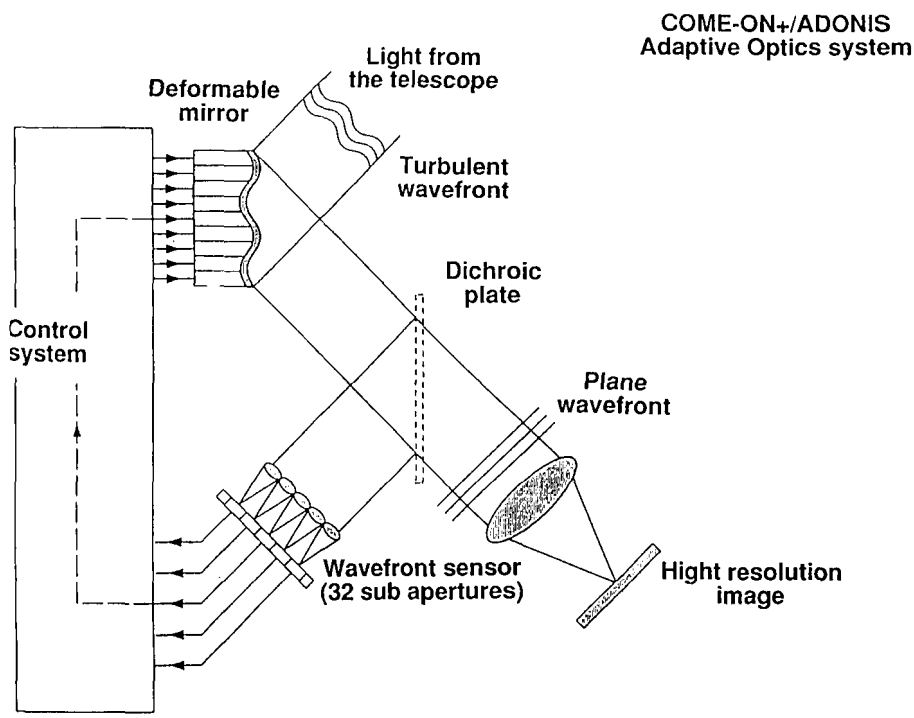

Figure 1: The COME ON+/ADONIS adaptive optics system.